The Effect of SPIO Nanoparticles Size on Transduction of PEGylated Lentiviral Vector

Hamed Omid
Sharif University of Technology
Amirhosein Paryab
Sharif University of Technology
Yasamin Nakhli
Sharif University of Technology
Kobra Moradzadeh
Tehran University of Medical sciences
Nasim Sajadi
Iran University of Medical Sciences
Hamid Reza Madaah Hosseini
Sharif University of Technology
Naser Ahmadbeigi (n-ahmadbeigi@tums.ac.ir)
TUMS: Tehran University of Medical Sciences

Research

Keywords: SPIO, Nanoparticles, Transduction, Gene editing, lentivirus, PEG

Posted Date: October 26th, 2021

DOI: https://doi.org/10.21203/rs.3.rs-981669/v1

Abstract

Gene editing has revealed many promising opportunities for the treatment of severe diseases including cancers and autoimmunes. There are two main routes for gene delivery: viral and non-viral. Recent research shows viral methods are very close to clinical trials. Nevertheless, there are a couple of obstacles to remove such as difficulty in virus concentration, low efficiency of transduction, and being time-consuming. In this work, by employing magnetic nanoparticles (NP) we tried to solve these problems. Conjugating these nanoparticles to viruses by polyethylene glycol (PEG) can increase sedimentation of viruses due to magnetic and gravity forces even without ultracentrifuge. Moreover, this magnetic force can guide viruses toward cells and tremendously facilitate the transduction process. Nanoparticle size has significant effects and should be considered for this application. As shown, average size nanoparticles revealed the best performance especially in combination with salting-out precipitation and increased transduction efficiency more than 20-fold.

Introduction

Genetics is one of the fast-growing fields with diverse promising visions including gene therapy. The gene inserting or eliminating that is known as gene-editing technology gives us the treatment ability of genetic disorders or maybe in the future the improvement of genomes. Many diseases do not respond to molecular therapy, and in turn, need cellular therapy with trained cells. The CAR-T cells developed by Yoshikazu Kuwana et al. in 1987 is an example of it [1].

There had been innumerable research in this field but getting the first FDA approval for gene-edited cells (KYMRIAH™, tisagenlecleucel) was a turning point. The initial use of gene-editing in people was in 2014 that the clinical trials of gene-edited cells were employed to treat HIV patients [2]. They used the zinc-finger nuclease (ZFN) enzyme in an ex vivo setup to cut out the gene responsible for the T cells' protein targeted by HIV. Then gene-edited T cells injected to the patients. This method revealed a promising opportunity for HIV treatment. Interestingly, in vivo gene editing also becomes possible. Sharma et al. in 2015 employed ZFN-mediated site-specific integration of transgenes by an adeno-associated viral (AAV) vector for long-term expression of human factors VIII ND IX in mouse models of hemophilia A and B [3].

There are several severe and prevalent diseases including cancers, autoimmune, and inherited diseases which can be cured by gene editing. Among transduction methods, viral vectors are much closer to clinical trials. However, some barriers cause low efficiency and slow kinetics for both transfection and transduction. One of these barriers is the low concentration of DNA at the cell surface [4] due to the high colloidal stability of viruses in biologic media and repulsive electric force on the cell membrane (both have a negative charge). To solve the problem, a range of solutions has been suggested including cationic ions, polymers, liposomes, needle injection, biolistic gun, electroporation, microfluidic, etc.

These methods were employed to deposit vectors on the cell surface. For years, researchers used straightforward techniques such as removing media before transduction, giving several incubation hours,

or raising MOI to increase viral vectors contact with cells. Nonetheless, they were not helpful for clinical trials. Removing media and incubation time are irrelevant to in vivo, and increasing MOI has tumor genesis issues. Moreover, one of the requirements of clinical trials is the large-scale production of viruses which is costly, and high MOI expends more. Hence, it's important to find an FDA approved method to increase the efficiency of transduction inexpensively without serious side effects.

Superparamagnetic iron oxide (SPIO) nanoparticle is well-known in medical and biological applications [5–7]. For the transfection process, superparamagnetic iron oxide (SPIO) nanoparticle was used which became well-known as the "magnetofection" method and revealed lots of promising results [8]. In this work, we employed SPIO NPs for the transduction process which had several advantages. First, the highly weighted metal oxide particles facilitated the viral concentration and eliminated the ultracentrifuge necessity. Second, magnetic forces could increase transduction efficiency and decrease its time immensely. Third, iron oxide NPs are FDA-approved and trackable in transduced cells by Magnetic resonance imaging (MRI) [7]. This work showed "magnetoduction", using magnetic NPs for transduction, is as fruitful as magnetofection.

Materials And Methods

1. Synthesis and PEG functionalization of magnetite nanoparticles

1.1. Materials

Iron (III) chloride hexahydrate ($FeCl_3.6H_2O$), Iron(II) chloride tetrahydrate ($FeCl_2.4H_2O$), sodium hydroxide (NaOH), potassium nitrate (KNO_3), Iron (II) sulfate heptahydrate (FeSO4.7H2O), potassium hydroxide (KOH), and polyethylene glycol -6000 (PEG) were all purchased from Merck and used without further treatment. 3-[4,5-dimethylthiazol-2-yl]-2,5-diphenyl tetrazolium bromide (MTT) was purchased from Sigma-Aldrich.

1.2. Co-precipitation synthesis of magnetite nanoparticles

Co-precipitation synthesis was done in order to provide 2 samples. Their processes are different in terms of reactant concentrations and base addition rate which leading to 2 samples namely NP1 and NP2. All steps were carried out at room temperature. First, 0.002 mol of FeCl3.6H2O and 0.001 mol of FeCl2.4H2O were dissolved in 10 mL (NP1) and 50 mL (NP2) DI water in two different beakers. Then, 0.008 mol of NaOH was dissolved in 10 mL (NP1) and 50 mL (NP2), separately. For the NP1 sample, the iron chloride solution was added to the base solution at the rate of 1mL/min and for the NP2 sample 5 mL of the base solution was added into the iron chloride solution every five minutes until it was finished. Both samples were magnetically decantated and washed once with ethanol and twice with DI water. The nanoparticles were dispersed in DI water and kept for subsequent treatment [9].

1.3. Sol-Gel synthesis on magnetite nanoparticles

This method was carried out according to the paper published by Sugimoto in 1979 [10]. First, DI water was bubbled by N2 gas in order for O2 in water to be eliminated. Then, 2 mL of 1.25 M KOH solution and 2 mL of 2 M KNO3 solution were prepared and added into a 50 mL volume three neck reactor. The reactor was heated to 50 ˚C in an oil bath. After 15 minutes, 6 mL of 0.0416 M FeSO4.7H2O solution was added to the reactor. At this moment a green precipitate was formed inside the reactor. The temperature was raised to 90 ˚C and the system was aged for 4 hours. The whole process was carried out in N2 gas purge. After synthesis, the nanoparticles were dispersed with ultrasound and centrifuged so that the unreacted ions could be freed from intraparticle voids. This treatment was done three times and the nanoparticles were kept in water for subsequent treatments.

1.4. PEG functionalization of nanoparticles

Synthesized nanoparticles were first dried at 60 ˚C for 72 hours. Then, 0.2 g of nanoparticles was taken and put into a beaker. Following that, 0.2 g of PEG and 30 mL of DI water were added into the same beaker and transferred to the ultrasound setup. The whole system was subjected to regular pulses for 5 minutes. After that, the nanoparticles were centrifuged and excess PEG was removed from the solution.

2. Characterization of nanoparticles

X-ray diffraction method was performed for phase analysis using XRD, Panalytical-2009, Cambridge, the U.K employing Cu Kα radiation (0.15418 nm). Scherrer method was employed in Phillips X'Pert Highscore. FT-IR test was carried out to investigate functional groups on the nanoparticles using a Bruker Vertex 70 FT-IR instrument (Bruker, USA). Field Emission Scanning Electron Microscope (FE-SEM, TeScan Mira III, Brno, Czech Republic) was used to study the morphology of the particles. Also, to study the magnetic properties of Fe3O4 nanoparticles a vibrating sample magnetometer (VSM) experiment was carried out with an HH15 apparatus between 10-4 and 104 G.

3. Cell lines and culture

The Lenti-X 293T cell line was purchased from the Iranian Biological Resource Center, Tehran, Iran. The Cells were cultured in high glucose Dulbecco's Modified Eagle's Medium (DMEM) with 10% fetal bovine serum (FBS) supplement, Streptomycin 100 µg/mL, and Penicillin (All from Gibco) under a humidified air with 5% CO2 at 37°C.

4. Lentiviral vector production

3×105 Lenti-X 293T cells were seeded in a T-25 flask and incubated at 37˚C, 5% CO2 for 24h. 21µg of three vectors (pCDH : pSPAX2 : pMD2.G = 2 : 2 : 1) were diluted in NaCl 150mM to reach total volume of 1.5mL. 10µL of PEI (40KD) was diluted in 40µL of NaCl 150mM and added 84µL of PEI solution to the vectors sample. After vortexing, the mixture incubated for 15 minutes at room temperature. The culture medium of the flask was removed and the prepared transfection solution added to it. New culture medium and serum added to flask 30 minutes after transfection. The lentiviral particles were collected

from supernatant at 24, 48, and 72h after transfection. The collected viral soups were pooled, filtered, and stored at -80˚C [11].

5. Magnetoduction

3×104 Lenti-X 293T cells were seeded in a 24-well plate and incubated for 24h. The mixture of NPs (0.5mg Fe) and 200µL PEG 50% after thorough sonication added to 1.5mL of prepared viral soup in a 2mL Eppendorf tube, then 50µL NaCl 5M added to the tube and shook for 6h in 4˚C. Afterward, the tube centrifuged for 20min at 4000g, 4˚C. For salting-out samples before centrifuge 100µL NaCl 5M was added. The supernatant was removed and the remnant was added to the cells without culture medium. After transducing cells for 2h, fresh medium added to wells and incubated for 3 days, then cells were ready for flow cytometry.

6. Flow cytometry

After transduction, the GFP (green fluorescent protein) percent of trypsinized cells can be measured by flow cytometry, Facscalibur, BD Biosciences-US. For accurate statistical calculation, the GFP percent should be lower than 30%. Lower GFP percentage eliminates the probability of multi-entrance of particles to a single cell. By decreasing viral soup volume, we can decline the GFP percent. According to equation (1), the number of viral particles per 1µL can be achieved statistically.

$$\text{Particle per } \mu\text{L} = \frac{\text{number of cells} * \text{GFP\%}}{\text{Viral soup vol } (\mu\text{L})} \qquad (1)$$

7. Cell Proliferation Assay

The viability of lenti-X 293 cells was assayed using MTT assay. Cells were incubated with viral soup, viral soup-PEG, and viral soup-PEG-NPs in a 96 well plate. Concentrations in the MTT assay were the same as the ones used in the transduction process. After 24h incubation at 37°C, mediums were replaced by 0.5mg/mL MTT solution. In the transduction process, cells exposed for 2h to this concentration, but for MTT assay exposure time extended to 24h to exaggerate cytotoxicity.

Results

1. Characterization of synthesized NPs

Figure 1 (A) shows the XRD patterns of the synthesized nanoparticles. The pattern is well-matched with the magnetite (Fe3O4) diffraction peaks (JCPDS card no. 19-0629) and confirms the inverse spinel structure in all samples. Obviously, by decreasing NPs size the intensity of peaks reduces [12]. Low

intensity and wider peaks increase full wide at half maximum (FWHM) that has reciprocal relation with crystalline size according to the Scherrer equation. These size results were in accordance with FE-SEM data.

FTIR spectra of PEG-6000 and unmodified nanoparticles are shown in figure 1 (B). The stretch and the vibration band of ether –C–O–C– are visible in the PEG spectrum at 1101 cm−1 and 1349.4 cm−1, respectively [13]. The 1464 cm−1 transmittance band attributes to the vibration of –CH2 [14] and the peak near 950 cm−1 corresponds to the out-of-plane bending vibration of –CH. The transmittance band at 578 cm−1 represents the stretching mode of Fe–O in Fe3O4 [15]. The wide peak of 3450 cm−1 in both spectra represents the attached hydroxyl groups [13]. In the SPION-PEG spectrum, the transmittance of ether stretch and –CH2 vibrational bands can confirm the existence of PEG on the particles' surface. This spectrum had a negligible shift rather than free PEG. Due to attaching the polymer to the surface of the particles, it shows lower frequencies [13].

FESEM micrograph and size dispersity of the synthesized samples were shown in figure 2. According to FESEM images, NPs' core sizes were measured and NP percentage in each interval was plotted. As presented 10, 40 and 120 nm are mode sizes in sample NP1, NP2, and NP3, respectively. Smaller NPs in the same concentration have a larger surface-to-volume ratio which increases surface energy and colloidal stability. Higher surface energy intensifies bounding tendency, and more stability increases the number of colloidal collisions between NPs and virus. Both of these parameters enhance virus fishing from the viral soup and improve the efficacy of viral concentrating without ultracentrifuge. However, higher surface energy increases the agglomeration of NPs and declines catching viruses. Smaller NPs have lower weight and lower gravity force to sediment viruses. Accordingly, the small size of NPs has advantages and disadvantages in this application, and this article revealed there is an optimum size for it.

Figure 2 represents hysteresis loops of iron oxide NPs by VSM. Sample NP1 shows perfect superparamagnetism and by increasing the size of NPs superparamagnetic behavior disappears. However, coercivity is still negligible in NP2 and NP3. Sample NP2 has the highest magnetization. In very large particles, the hysteresis loop area increases which means these particles can save magnetism. This remaining magnetism causes higher attraction force and more agglomeration. Hence, NP2 seems to have optimum magnetic behavior, higher magnetization, and lower coercivity which concluded to higher response to the magnetic field and higher colloidal stability.

2. Binding ability of NP to the lentivirus

Due to the high surface energy of NPs, some of them bind to the viruses and increase transduction efficacy by about %50. In figure 3, V is the viral soup sample and V-NP1 is a mixture of viral soup with NP1 sample, and V-NP1 is 1.5 fold of V. However, PEG has a much better binding ability to viruses and shows near 6-fold improvement rather than the V sample. Hence, PEG was used to increase the binding between NPs and viruses and revealed a synergic effect more than 11-fold (V-PEG-NP1).

3. Evaluating transduction efficiency with GFP expression

Figure 4 reveals flow cytometry results for the transduction process by three different NP sizes and salting-out method in similar condition. Figure 4 (A) shows the GFP expression of transduced cells by 50μL centrifuged viral soup. Figure 4 (B, D, F) represents the results of transduction by 3μL centrifuged virus, PEG, and NP complex, and figure 4 (C, E, G) shows the salting-out method of these three complexes. Obviously, NP2 (figure 4 D and E) shows higher GFP expression, and the NP3 complex (figure 4 F and G) was the worse one. The salting-out method had a good synergic on NP1 and NP2 by accelerating sedimentation of virus-PEG-NP complex but made NP3 sample worse.

4. Targeted gene delivery

Magnetic NPs in addition to efficacy enhancement of the transduction are able to deliver the vector to a specific area. This control would be worthwhile particularly in in-vivo gene delivery.

As shown in figure 5, in areas with most NPs accumulation there is more GFP expression. Due to the attachment of viruses to NPs, areas with NPs aggregate are enriched virus ones and have a higher probability of transduced cells.

5. Effect of NPs' size

Comparison of magnetoduction with three different sizes of NPs revealed that size has undeniable roles on the efficiency of transduction. White columns in figure 6 represent NP2 with 40nm average size has the highest efficiency, around 1100%. NP1 with the best stability but lowest weight and magnetic force has the second position. The largest sample (NP3) due to low colloidal stability has the worst result. The grey columns are the salting-out method and exhibit a synergic effect on NP1 and NP2. Increasing ion strength can destabilize the colloidal system and accelerate sedimentation of the V-PEG-NP complex. By contrast, its antipathy on NP3 is obvious. NP3 is the unstable one and salting-out makes it worth, and rapid sedimentation of NPs prevents collision and attachment between viruses and NPs. It can be concluded the combination of NP with average size and salting-out method is the best option for magnetoduction that increases the efficiency more than 20-fold.

6. Cytotoxicity of magnetoduction

MTT assay (figure 7) revealed that neither lentivirus, PEG nor NPs have significant cytotoxicity on the Lenti-X293T cells after 24h. However, the NP2 and NP3 samples declined the cell proliferation to about 90% and 80%, respectively. In the transduction process, a new culture medium can be added after 2h that eliminates most of the NPs and just NPs which entered cells remain. Hence, the toxicity of NPs doesn't cause serious concern.

Discussion

Nanosize viruses have good stability in media and it is difficult to concentrate them without employing ultracentrifuge. In very high G-force, the exerted shear stress on viruses increases tremendously which can damage them. There is a large number of researches on eliminating ultracentrifuge necessity [16, 17].

Wei Jiang et al. [18] revealed that due to the fragile nature of lentivirus not only high G-force but also acceleration or brake speed can damage them significantly. However, using heavy metallic NPs and magnetic force can accelerate the sedimentation of viruses without any harm. Moreover, putting out samples from ultracentrifuge and carrying them have enough shaking to lose some portion of them that would be costly in the large-scale application. But attaching the virus to magnetic NP gives us the ability to concentrate them anytime, and the polymeric net of PEG minimizes the virus loss. Being time-effective and inexpensive makes this method suitable for clinical trials.

NP1 has a small size and high stability, therefore it can catch viruses better, and using the salting-out method for these particles shows huge improvement. On the other hand, NP3 has the largest size and lowest stability. Hence, the salting-out method makes its stability worse and decreases virus fishing. Finally, the NP2 sample with average size revealed the best performance. It has both stability and weight to fish viruses and concentrates them.

Conclusion

Our results indicated that the size of NPs has a vital role in the efficiency of magnetoduction. For transduction of HEK 293T cells by lentivirus, iron oxide NP with an average size of 40nm had a greater outcome, and combining it with the salting-out method showed a synergistic effect. These NPs are FDA approved and suitable for clinical trials. On the other hand, they are inexpensive in comparison to other methods which makes them appropriate for large-scale applications. The magnetic force of these NPs precipitates viruses to cells and improves the efficiency of transduction even in low MOIs. Low MOI decreases virus consumption and lowers expenses of therapy and reduce tumor genesis side effect of high gene loads.

Declarations

Ethics approval and consent to participate

Not applicable

Consent for publication

Not applicable

Availability of data and materials

Not applicable

Competing interests

The author(s) declare(s) that they have no competing interests

Funding

This work was supported by the Gene Therapy Research Center, Digestive Disease Research Institute, Tehran University of Medical Sciences, Tehran, Iran.

Authors' contributions

Not applicable

Acknowledgements

Not applicable

References

[1] Y. Kuwana, Y. Asakura, N. Utsunomiya, M. Nakanishi, Y. Arata, S. Itoh, F. Nagase, and Y. Kurosawa, “Expression of chimeric receptor composed of immunoglobulin-derived V regions and T-cell receptor-derived C regions,” *Biochem. Biophys. Res. Commun.*, vol. 149, no. 3, pp. 960–968, Dec. 1987. https://linkinghub.elsevier.com/retrieve/pii/0006291X8790502X

[2] P. Tebas, D. Stein, W. W. Tang, I. Frank, S. Q. Wang, G. Lee, S. K. Spratt, R. T. Surosky, M. A. Giedlin, G. Nichol, M. C. Holmes, P. D. Gregory, D. G. Ando, M. Kalos, R. G. Collman, G. Binder-Scholl, G. Plesa, W.-T. Hwang, B. L. Levine, and C. H. June, “ Gene Editing of CCR5 in Autologous CD4 T Cells of Persons Infected with HIV,” *N. Engl. J. Med.*, vol. 370, no. 10, pp. 901–910, Mar. 2014. https://www.nejm.org/doi/full/10.1056/nejmoa1300662

[3] R. Sharma, X. M. Anguela, Y. Doyon, T. Wechsler, R. C. DeKelver, S. Sproul, D. E. Paschon, J. C. Miller, R. J. Davidson, D. Shivak, S. Zhou, J. Rieders, P. D. Gregory, M. C. Holmes, E. J. Rebar, and K. A. High, “In vivo genome editing of the albumin locus as a platform for protein replacement therapy,” *Blood*, vol. 126, no. 15, pp. 1777–1784, Oct. 2015. https://pubmed.ncbi.nlm.nih.gov/26297739/

[4] D. Luo and W. M. Saltzman, “Enhancement of transfection by physical concentration of DNA at the cell surface,” *Nat. Biotechnol.*, vol. 18, no. 8, pp. 893–895, Aug. 2000. http://www.nature.com/articles/nbt0800_893

[5] M. Mahmoudi, S. Sant, B. Wang, S. Laurent, and T. Sen, “Superparamagnetic iron oxide nanoparticles (SPIONs): Development, surface modification and applications in chemotherapy,” *Adv. Drug Deliv. Rev.*, vol. 63, no. 1–2, pp. 24–46, 2011. https://doi.org/10.1016/j.addr.2010.05.006

[6] Emilie Allard-Vannier, Katel Hervé-Aubert Karine Kaaki, Thibaut Blondy, Anastasia Shebanova, Konstantin V. Shaitan, Anastasia A. Ignatova, Marie-Louise Saboungi, Alexey V. Feofanov, and Igor Chourpa, “Folic acid-capped PEGylated magnetic nanoparticles enter cancer cells mostly via clathrin-dependent endocytosis”, *Biochimica et Biophysica Acta (BBA) - General Subjects*, vol. 1861, pp. 1578-1586, June 2017. https://doi.org/10.1016/j.bbagen.2016.11.045

[7] R. Ahmadi, H. R. M. Hosseini, A. Masoudi, H. Omid, R. Namivandi-Zangeneh, M. Ahmadi, Z. Ahmadi, and N. Gu, “Effect of concentration on hydrodynamic size of magnetite-based ferrofluid as a potential MRI contrast agent,” *Colloids Surfaces A Physicochem. Eng. Asp.*, vol. 424, no. 0, pp. 113–117, May 2013. https://doi.org/10.1016/j.colsurfa.2012.11.069

[8] F. Scherer, M. Anton, U. Schillinger, J. Henke, C. Bergemann, A. Krüger, B. Gänsbacher, and C. Plank, “Magnetofection: Enhancing and targeting gene delivery by magnetic force in vitro and in vivo,” *Gene Ther.*, vol. 9, no. 2, pp. 102–109, 2002. https://doi.org/10.1038/sj.gt.3301624

[9] T. Iwasaki, N. Mizutani, S. Watano, T. Yanagida, and T. Kawai, “Size control of magnetite nanoparticles by organic solvent-free chemical coprecipitation at room temperature,” *J. Exp. Nanosci.*, vol. 5, no. 3, pp. 251–262, Jun. 2010. https://doi.org/10.1080/17458080903490731

[10] T. Sugimoto and E. Matijević, “Formation of uniform spherical magnetite particles by crystallization from ferrous hydroxide gels,” *J. Colloid Interface Sci.*, vol. 74, no. 1, pp. 227–243, Mar. 1980. https://doi.org/10.1016/0021-9797(80)90187-3

[11] Y. Gheisari, K. Azadmanesh, N. Ahmadbeigi, S. M. Nassiri, A. F. Golestaneh, M. Naderi, M. Vasei, E. Arefian, S. Mirab-Samiee, A. Shafiee, M. Soleimani, and S. Zeinali, “Genetic Modification of Mesenchymal Stem Cells to Overexpress *CXCR4* and *CXCR7* Does Not Improve the Homing and Therapeutic Potentials of These Cells in Experimental Acute Kidney Injury,” *Stem Cells Dev.*, vol. 21, no. 16, pp. 2969–2980, Nov. 2012. https://doi.org/10.1089/scd.2011.0588

[12] B. Cullity, *Elements of x-ray diffraction*, Second edition. Reading MA: Addison-Wesley Publishing Company Inc., 1978.

[13] A. K. Gupta and S. Wells, “Surface-Modified Superparamagnetic Nanoparticles for Drug Delivery: Preparation, Characterization, and Cytotoxicity Studies,” *IEEE Trans. Nanobioscience*, vol. 3, no. 1, pp. 66–73, Mar. 2004. https://doi.org/10.1109/TNB.2003.820277

[14] L. Hu, D. Hach, D. Chaumont, C. H. Brachais, and J. P. Couvercelle, “One step grafting of monomethoxy poly(ethylene glycol) during synthesis of maghemite nanoparticles in aqueous medium,” *Colloids and Surfaces A: Physicochemical and Engineering Aspects*, vol. 330, no. 1. Elsevier, pp. 1–7, 20-Nov-2008. https://doi.org/10.1016/j.colsurfa.2008.07.044

[15] M. Kim, J. Jung, J. Lee, K. Na, S. Park, and J. Hyun, “Amphiphilic comblike polymers enhance the colloidal stability of Fe3O4 nanoparticles,” *Colloids Surfaces B Biointerfaces*, vol. 76, no. 1, pp. 236–240,

Mar. 2010. https://doi.org/10.1016/j.colsurfb.2009.10.042

[16] “Lentivirus Gene Engineering Protocols | Maurizio Federico | Springer.” [Online]. Available: https://www.springer.com/gp/book/9781607615323. [Accessed: 08-Jan-2021].

[17] K. Yamada, D. M. McCarty, V. J. Madden, and C. E. Walsh, “Lentivirus vector purification using anion exchange HPLC leads to improved gene transfer,” *Biotechniques*, vol. 34, no. 5, pp. 1074–1080, May 2003. DOI: 10.2144/03345dd04

[18] W. Jiang, R. Hua, M. Wei, C. Li, Z. Qiu, X. Yang, and C. Zhang, “An optimized method for high-titer lentivirus preparations without ultracentrifugation,” *Sci. Rep.*, vol. 5, no. 1, pp. 1–9, Sep. 2015. DOI: 10.1038/srep13875 (2015).

Tables

Table 1: Summary of samples properties.

Samples	Preparation Method	size (nm)	Magnetization (emu/g)
NP1	Co-precipitation	10	35.83
NP2	Co-precipitation	40	56.11
NP3	Sol-Gel	120	45.36

Figures

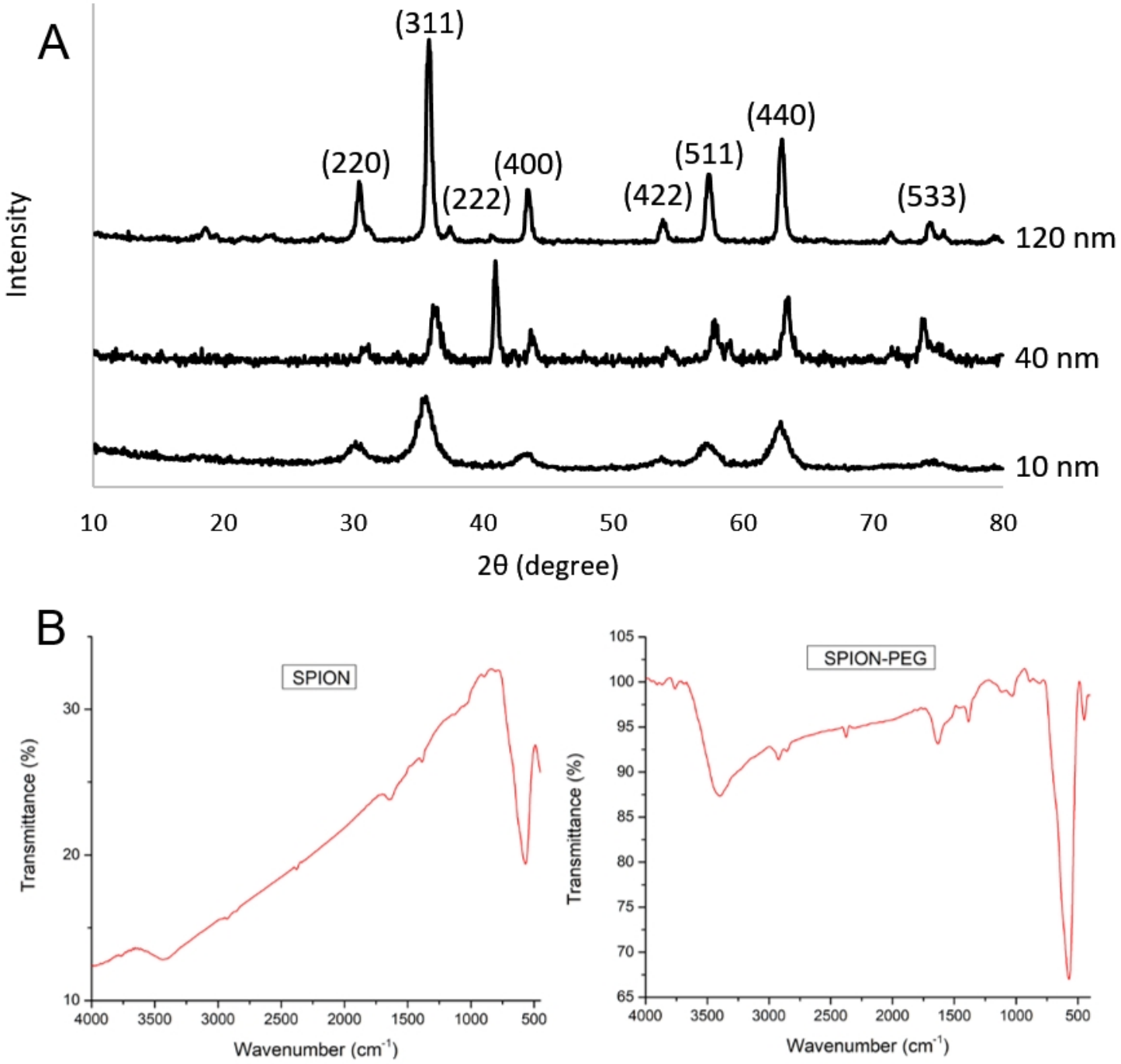

Figure 1

XRD pattern of synthesized 10, 40 and 120 nm Iron oxide particles (A), and FTIR spectrum of SPION and SPION-PEG (B).

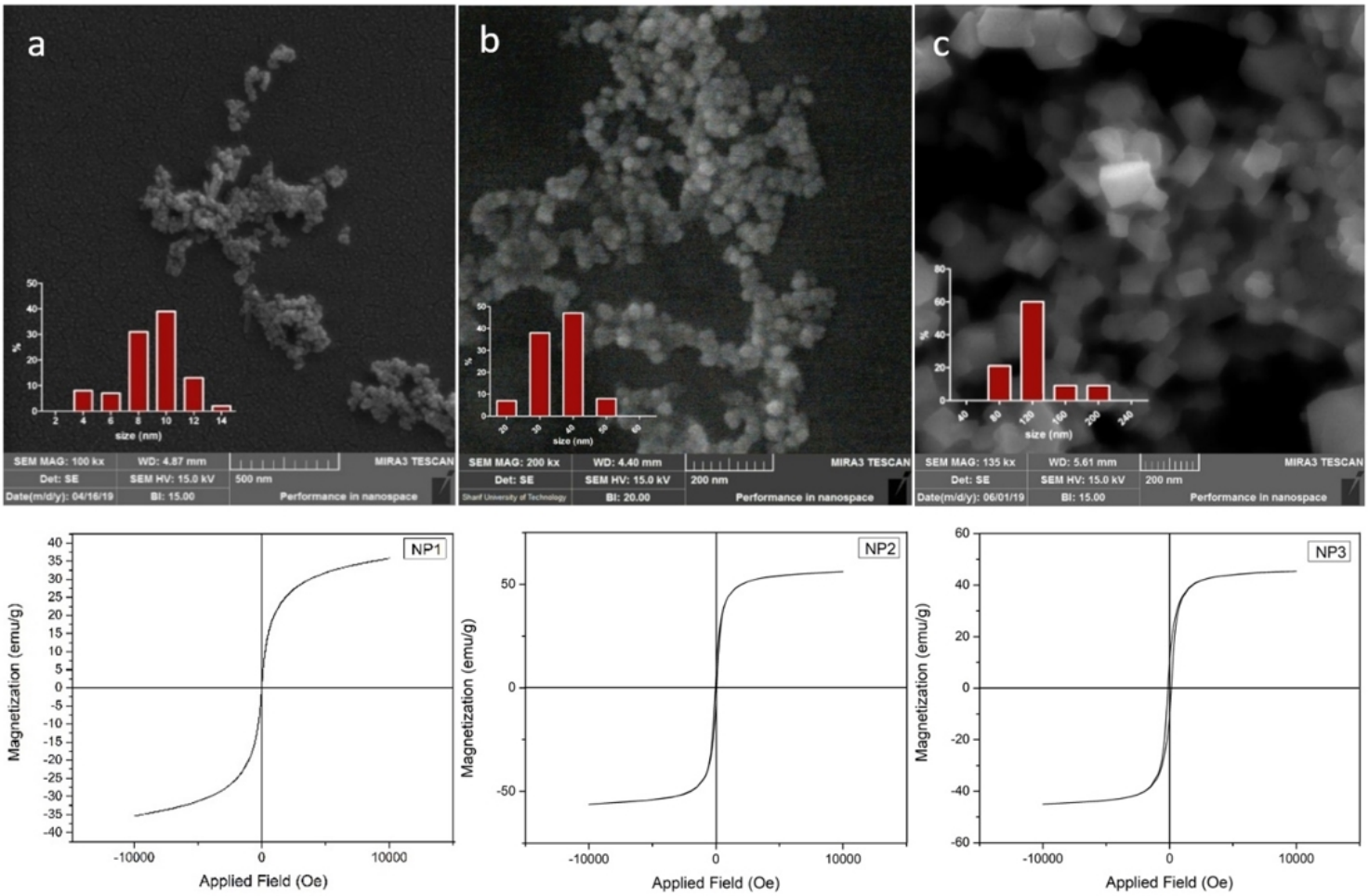

Figure 2

FESEM micrographs with size dispersity plots and VSM results of the synthesized NPs.

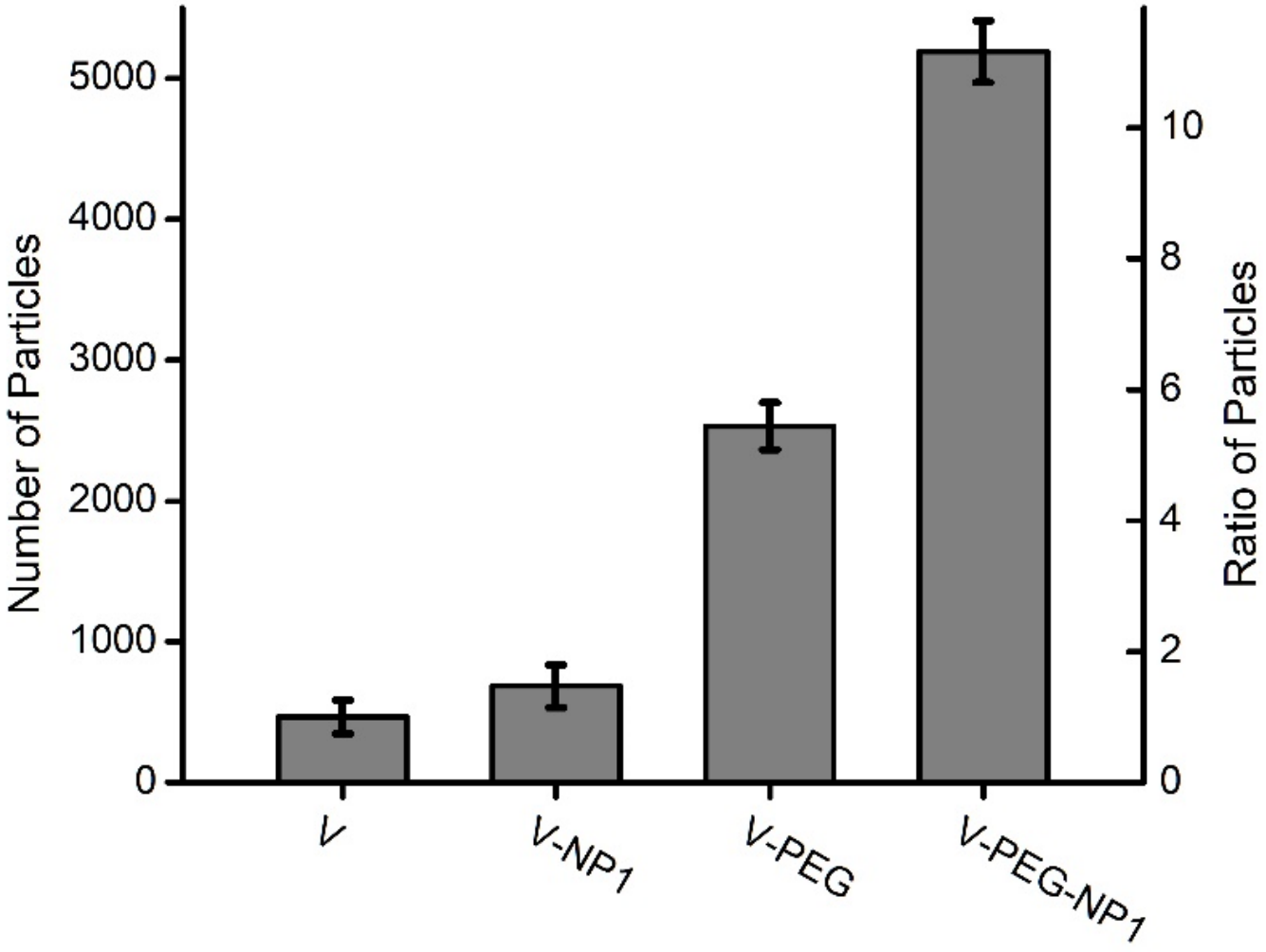

Figure 3

Number of Viral particles that successfully entered cells in transduction process. V, V-NP1, V-PEG and V-PEG-NP1 are mere viral soup, mixture of viral soup and NP1 sample, mixture of viral soup and PEG, and mixture of viral soup, PEG and NP1, respectively.

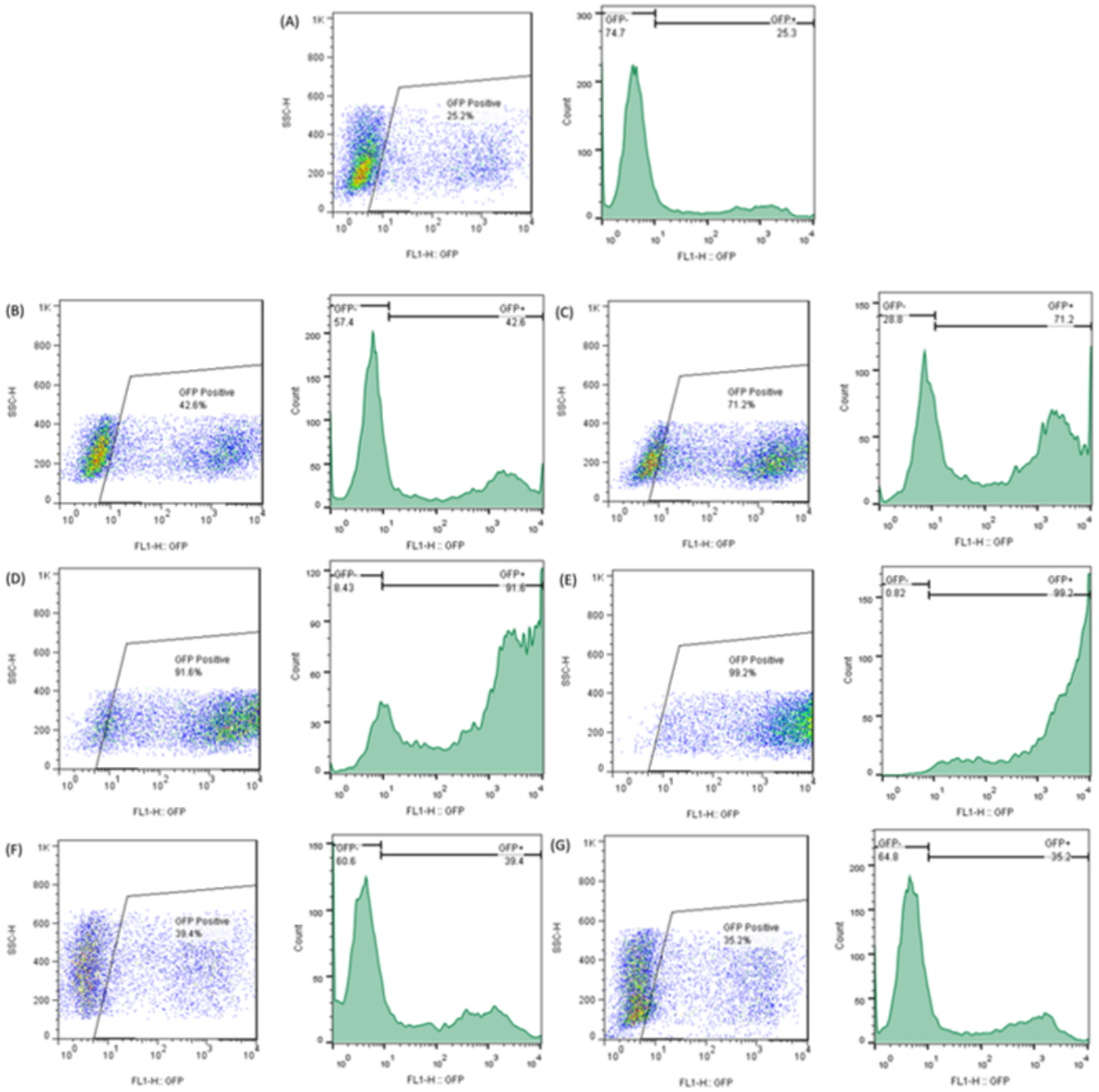

Figure 4

Measurement of GFP expression in Lenti-X293T cells by flow cytometry. Transduction was done by mere viral soup (A), NP1 (B), NP1+S (C), NP2 (D), NP2+S (E), NP3 (F), NP3+S (G). For B-G, complexes of 3µL viral soup, PEG, and NP was used. E, F and G are salting out (+S) of B, C and D, respectively.

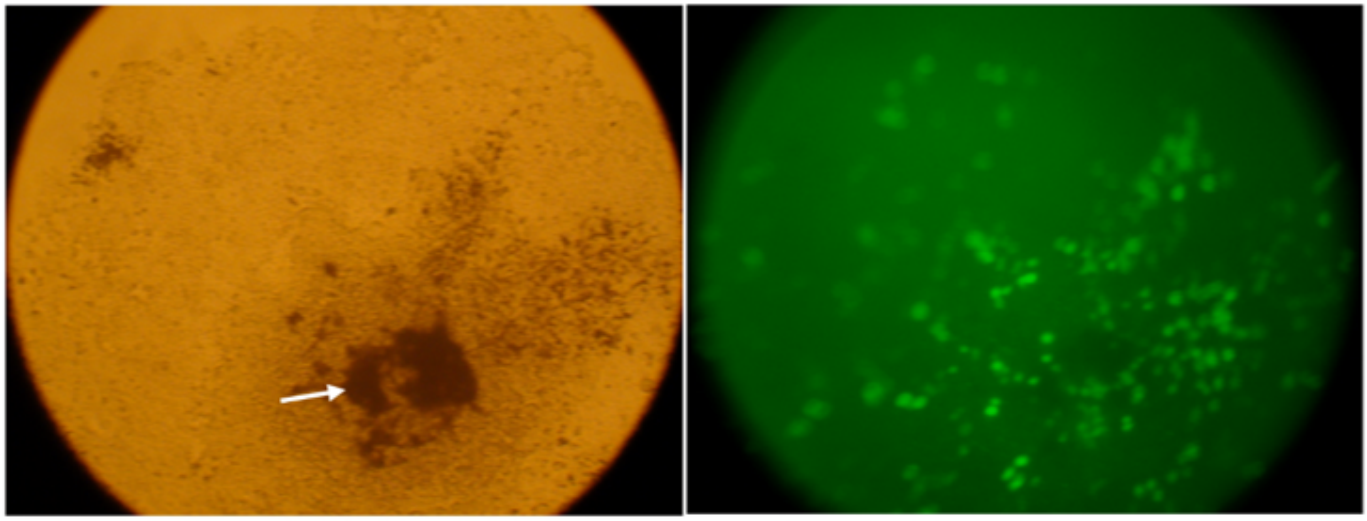

Figure 5

Optical microscopic image of Lenti-X 293T cells after transduction (Left), the dark spots are iron oxide NPs agglomeration. GFP expression in Lenti-X 293T 72h after magnetoduction under fluorescence microscopy (Right).

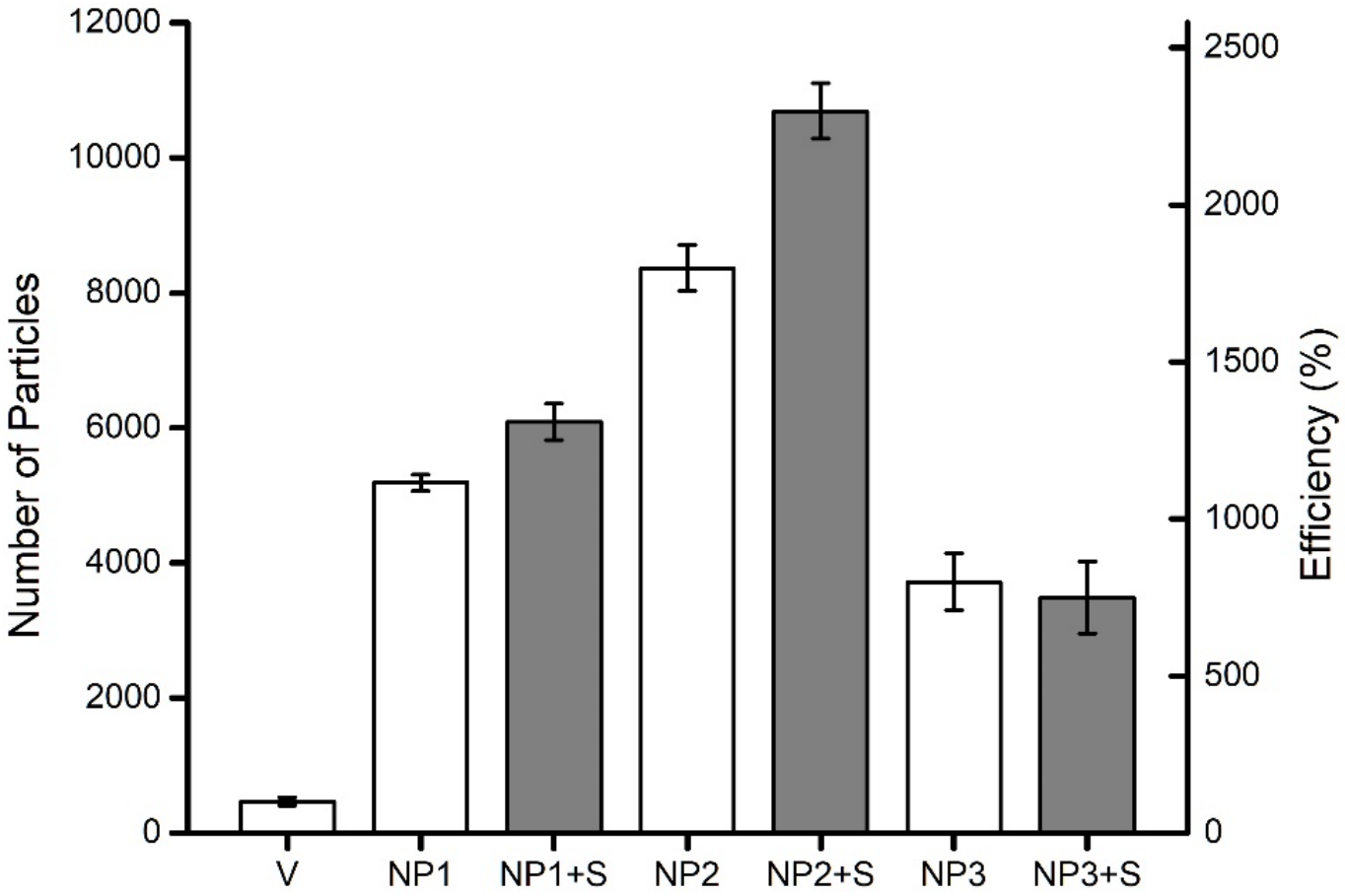

Figure 6

Efficiency of magnetoduction by NP1, NP2 and NP3 with and without salting out.

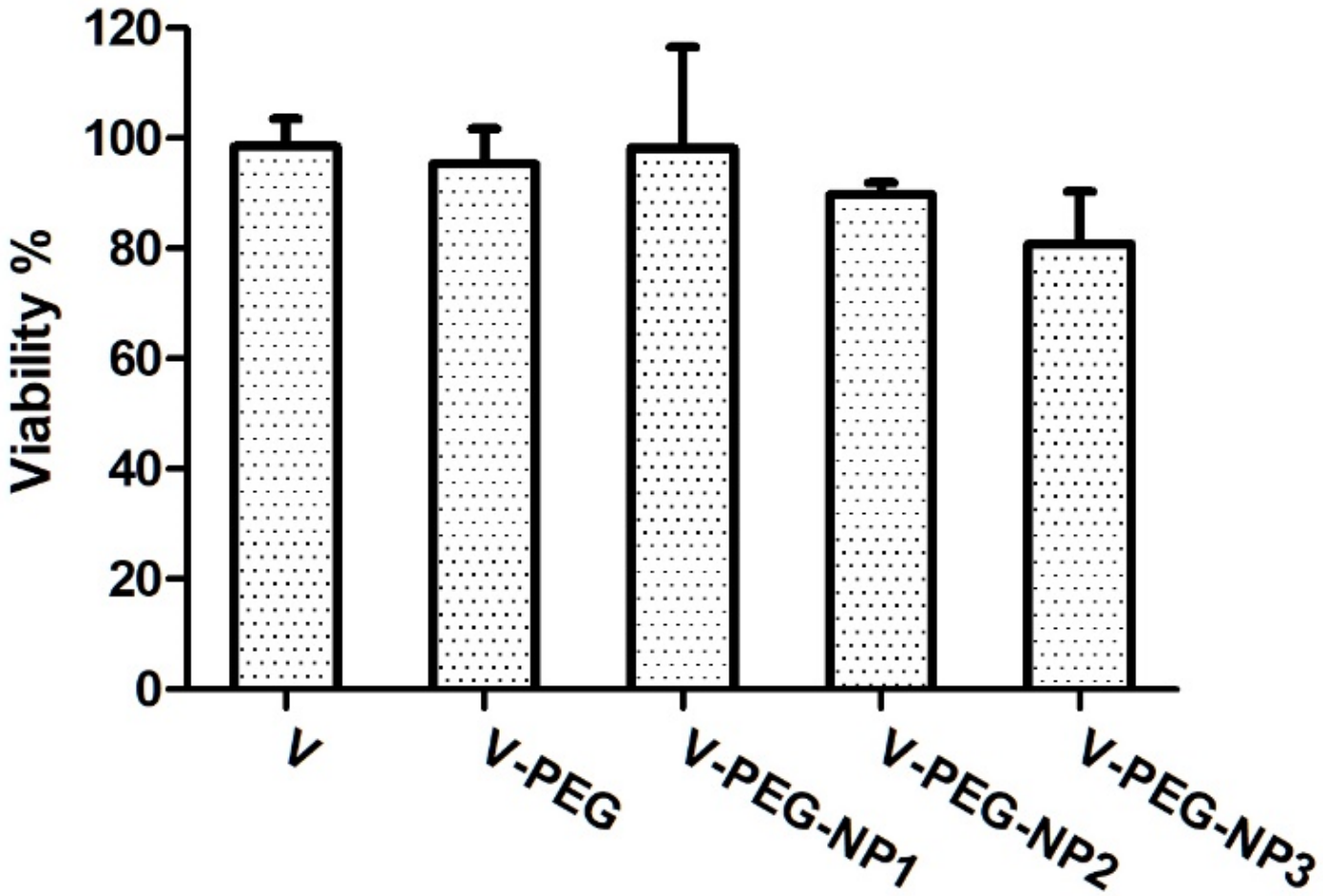

Figure 7

Viability of Lenti-X 293T cell line treated with viral soup (V), viral soup and PEG (V-PEG), and finally viral soup, PEG and NP samples (V-PEG-NP1 to 3) at 24h.

Supplementary Files

This is a list of supplementary files associated with this preprint. Click to download.

- GraphicalAbstract.docx